JOURNAL OF CATALYSIS **172,** 247–251 (1997)
ARTICLE NO. CA971808

RESEARCH NOTE

A New Application of Atomic Force Microscopy: The Visualization of Coke on Selective Oxidation Catalysts

Eric M. Gaigneaux,[1] P. Ruiz, E. E. Wolf,[2] and B. Delmon

Unité de Catalyse et Chimie des Matériaux Divisés, Université Catholique de Louvain Place Croix du Sud 2/17, B-1348 Louvain-la-Neuve, Belgium

Received February 18, 1997; revised May 16, 1997; accepted June 23, 1997

Coke frequently forms on the surface of catalysts used in many different reactions, including the hydroprocessing of petroleum fractions and pyrolysis oils and the selective oxidation of light alkanes and olefins. By remaining adsorbed on the surface, coke precludes the reactants from reaching the active sites, thus leading to deactivation. Many studies have focused on the determination of the nature of coke, of its formation mechanism, and on the elaboration of new catalyst formulations for minimizing its deposition (1–5). However, until now, except for a recent paper from McIntyre *et al*. (6), observing coke on Pt(111) clusters by scanning tunneling microscopy, and except for coke in an advanced stage of aromatization, observed by high resolution electron microscopy (7), the formation of coke precursors and amorphous coke has only been detected using "nonvisual" techniques like infrared or X-ray photoelectron spectroscopies.

In this work, atomic force microscopy (AFM) has been used to show directly, in a very "visual" way, what coke looks like when formed on the surface of oxidation catalysts, in particular, on MoO_3-containing catalysts used in the selective oxidation of isobutene to methacrolein. As a nonanalytical technique, AFM cannot confirm *a priori* whether topographic elements found on the surface of the samples are coke. However, this Note also aims at showing that this nonanalytical limitation can be circumvented by developing special strategies of investigation based on arguments from the literature. This opens new perspectives for AFM applications in many fields, particularly in catalysis. The strategy followed here consisted of analyzing samples, or zones of samples, where coke was or was not suspected of being present. The bibliographic supports were (i) the "structural specificities" of MoO_3 and (ii) the inhibiting effect exerted by α-Sb_2O_4 on the formation of coke. (i) The different faces of MoO_3 crystallites exhibit different characteristics and properties. Among others, the (010) faces preferentially perform deeper oxidation of hydrocarbons (mainly total oxidation) than the (100) faces (which are more selective to partially oxygenated products) (8–12). The (010) faces are thus more susceptible to the formation of −COOH residues than the (100) faces. These residues are an origin of surface carbonate coke precursors (13). Another point is that (100) faces are much more active than (010) faces. The superficial concentration of hydrocarbon is thus much lower on (100) than on (010). Hence, due to diffusion aspects, the middle of the (010) face should present the highest concentration of hydrocarbon, whereas a decreasing concentration should be observed when getting closer to the edges of the (100) faces. As coke formation is directly connected to the concentration of hydrocarbon, the prediction was that the extent of the coke deposition should be maximal in the center of the (010) faces of MoO_3 crystals, whereas it should progressively decrease when getting closer to the edges with the (100) faces ("inactive" for this type of coke formation). (ii) Zhou and Delmon showed that the elimination in air of coke from an artificially coked MoO_3 was accelerated when performed in the presence of α-Sb_2O_4 (14). Reversely, Li *et al*. observed that the formation of coke on SnO_2 in the oxidation of isobutene was dramatically inhibited when α-Sb_2O_4 was added to the active phase (13). Our second speculation was thus that MoO_3 crystals reacted in the oxidation of isobutene should be less coked when used in mixtures with α-Sb_2O_4 than when they are reacted alone.

The AFM analysis was performed on samples prepared intentionally to benefit from the facts and speculations mentioned above. Macroscopic MoO_3 monocrystals were prepared by condensation of a vapor of commercial molybdenum trioxide (BDH Chemicals, 99.5+%) obtained at 795°C in pure O_2 (Air Liquide, 99.995%). XRD and SEM characterizations showed that the obtained sample corresponded to the molybdite phase and that the (010) faces of the crystals were preferentially developed with dimensions

[1] "Aspirant" fellow for the Fonds National de la Recherche Scientifique of Belgium.

[2] Present address: Chemical Engineering Department, University of Notre Dame, IN 46556.

0021-9517/97 $25.00

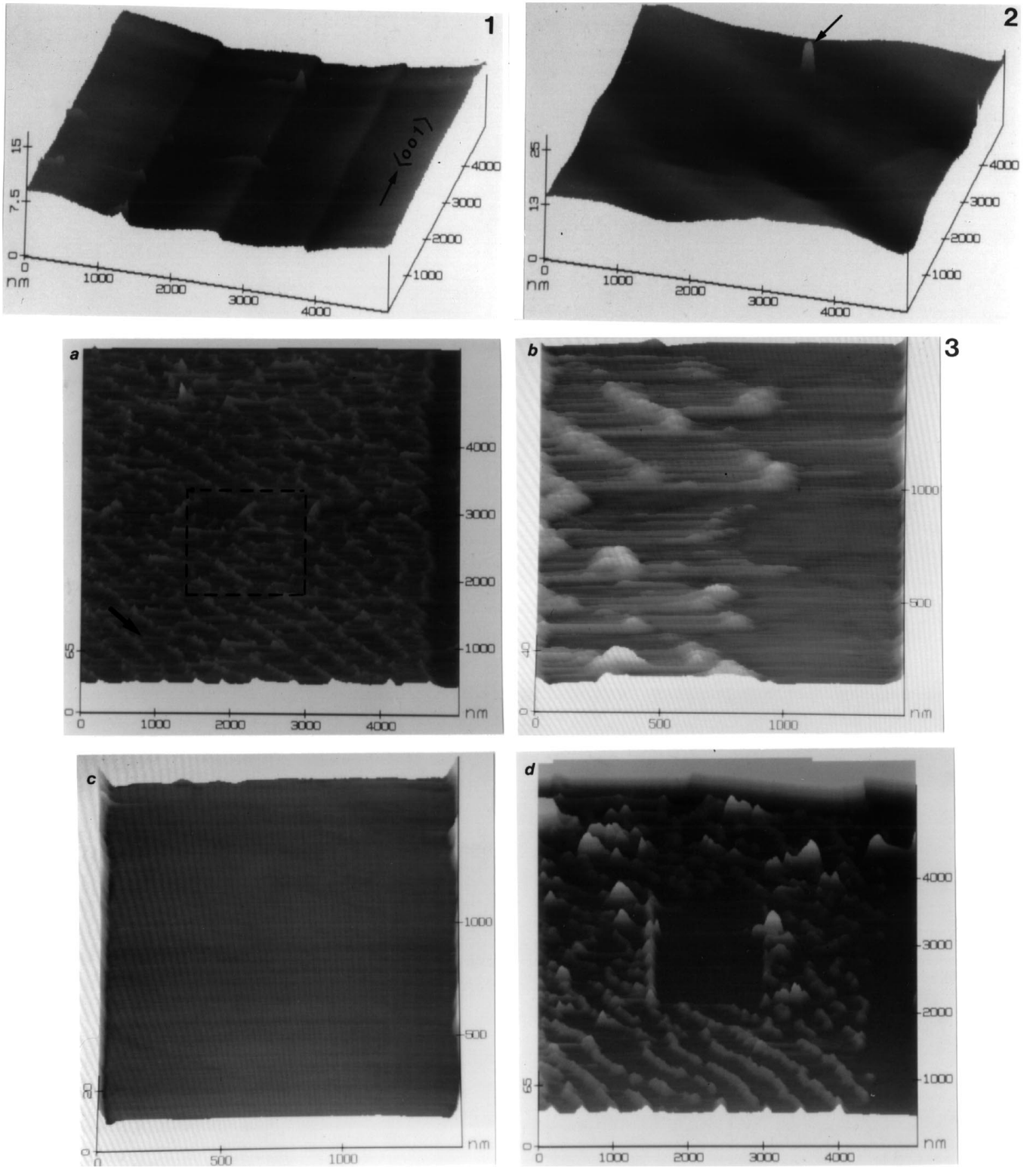
1
(001)
15
7.5
0
nm
1000
2000
3000
4000
2
25
13
0
nm
1000
2000
3000
4000
a
65
0
1000
2000
3000
4000
nm
b
3
40
0
500
1000
nm
c
20
0
500
1000
nm
d
65
0
1000
2000
3000
4000
nm

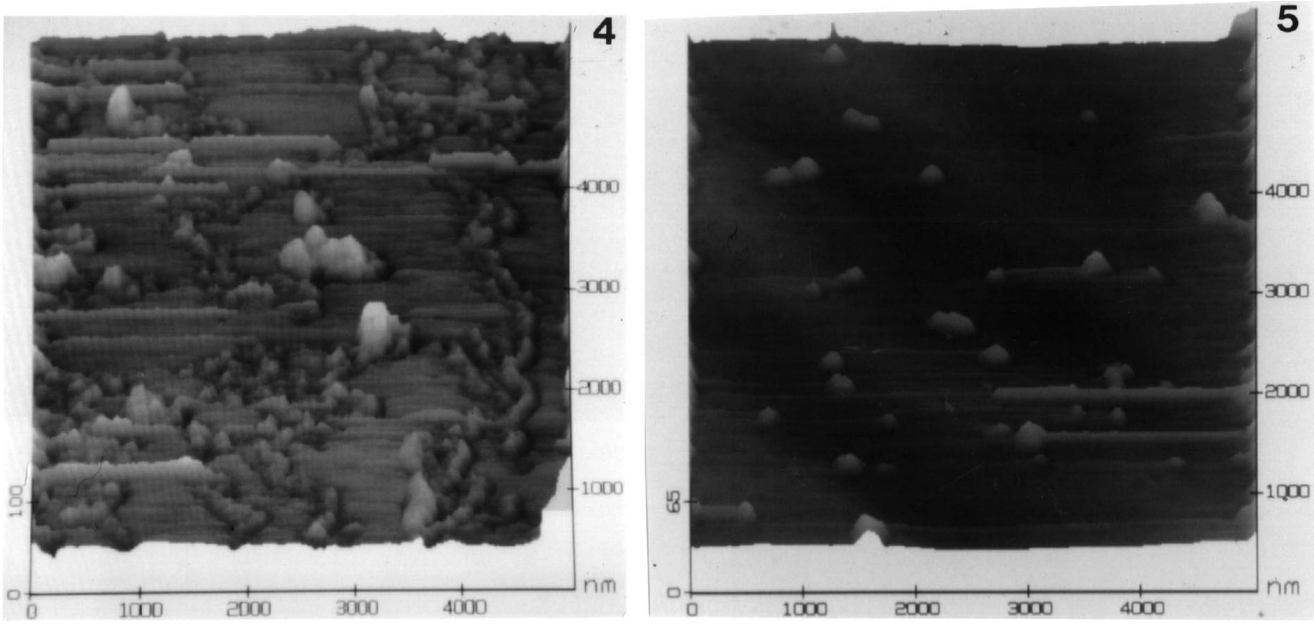

FIG. 4. A 5-μm AFM image of the (010) face in the proximity of the edge with the (100) face of a MoO_3 monocrystal after catalytic reaction in the absence of α-Sb_2O_4.

FIG. 5. A 5-μm AFM image of the middle of the (010) face of a MoO_3 monocrystal after catalytic reaction in the presence of α-Sb_2O_4.

ranging from 1 to 2 cm in the [001] direction and from 2 to 5 mm in the [100] direction, with a thickness ([010] direction) of about 3 μm. Powder α-Sb_2O_4 (cervantite phase) was synthesized by calcination (450°C/20 h) of commercial Sb_2O_3 (Aldrich, 99+%) previously dispersed in nitric acid (UCB, 70+% p.a.), washed with distilled water, and dried in air overnight (110°C). Particles of α-Sb_2O_4 were deposited on the (010) faces of the MoO_3 crystals by spreading some droplets of a 12.5 $g \cdot l^{-1}$ suspension in *n*-pentane. Pentane was therafter evaporated at room temperature. The success of the deposition was checked by optical microscopy. To make the comparison rigorous, the MoO_3 crystals to be used in the absence of α-Sb_2O_4 only received a few droplets of pure *n*-pentane. The catalytic reaction was performed with MoO_3 both in the absence and in the presence of α-Sb_2O_4, in a horizontal bed reactor. The gas mixture was isobutene/O_2/He = 1/2/7 (vol), with a total flow of 30 $ml \cdot min^{-1}$. The reaction was run at 420°C for 3 h. Heating and cooling before and after the reaction were done at 7.5°C $\cdot$ min^{-1} in the reaction gas. When cooled down, the samples were stored in Ar before AFM analysis. AFM was realized in air with a Digital Instruments Nanoscope-II microscope operating in contact mode on a bungee cord device. Before use, pyramidal (1 : 1 aspect ratio) Si_3N_4 tips were selected on the basis of the quality of the atomic resolution of mica they provided. The force constant of the cantilevers was 0.12 $N \cdot m^{-1}$. The scan rate was 2 Hz. The contact force was kept as low as possible (only slightly higher than the level of the baseline of the force curve). The possibility of artifact imaging was discarded systematically by varying the scan angle and checking the coherence of the consequent modification of the orientation of the image. No filtering of the images was applied. Analysis was performed on fresh MoO_3 both with and without α-Sb_2O_4 and on the corresponding samples after use in the catalytic reaction. Analyses were performed rapidly enough (only a few minutes for each sample) to allow to assume that the samples exposed to air at room temperature were not modified during the measurement. All the images presented hereafter are representative, in the sense that they correspond

FIG. 1. A 5-μm AFM image of the (010) face of a fresh MoO_3 monocrystal.

FIG. 2. A 5-μm AFM image of the (010) face of a fresh MoO_3 monocrystal covered with α-Sb_2O_4 particles. The arrow indicates an α-Sb_2O_4 particle.

FIG. 3. Sequence of the first four consecutive images of the (010) face of a MoO_3 monocrystal after catalytic reaction in the absence of α-Sb_2O_4. (a) First, 5-μm scan in a previously nonscanned area (the arrow indicates the [101] direction); (b) second, 1500-nm scan, zooming in the square shown in (a); (c) third, 1500-nm scan, same zone as (b); (d) fourth, 5-μm scan, zooming out in the same zone as (a).

to a selection made after a careful "statistical" investigation, checking the occurrence of observed features at different places on the samples, and on different crystals.

The (010) faces of fresh MoO_3 monocrystals, with and without particles of α-Sb_2O_4, presented very flat and smooth profiles with topographic irregularities within the range of the equipment noise (about 0.1 nm). For the crystals well developed in the [100] direction, sharp steps were observed parallel to the [001] direction, with heights ranging from 2.5 to 4 nm. These very likely corresponded to cleavage breaks (Fig. 1). For the monocrystals covered with antimony oxide, only very few particles (those smaller) of α-Sb_2O_4 were detected (Fig. 2). Most of these particles, composed of crystal agglomerates of about 2 μm (evaluated by SEM), were swept out of the scanned area by the tip during the scanning process. For both samples, no difference was distinguishable when scanning in the middle of the (010) faces or near the edges between these and the (100) faces.

After catalytic reaction in the absence of α-Sb_2O_4, the (010) faces of the MoO_3 crystals were decorated by an organized network of small balls. These were not observed on the fresh samples. The balls presented a diameter of approximately 10 nm (evaluated from their height) and were aligned in regular strings parallel to the [101] direction (Fig. 3a). These were adsorbed very loosely on the surface. Even during the first scan, the balls were displaced by the tip, and so imaged as tapered features. This is further shown in Figs. 3a–3d showing a sequence of the first four consecutive scans in the same ball-covered area. After the third scan, the zoomed square was completely cleaned of all the balls detected in the first passage. Conversely, when zooming out in the initial area, the borders of the inner square were covered by high piles of material, namely, the balls swept out of the scanned square.

When scanning the same crystals close to the edges between the (010) and the (100) crystallographic faces, identical balls were observed, but in amounts lower (at the first passage of the tip) than when scanning in the middle of the (010) faces. Also, the orientation of the rows of balls appeared to be disturbed compared with the middle of (010) (Fig. 4). The disorganization of the rows and the decrease in the number of balls were even more obvious when MoO_3 was reacted in the presence of α-Sb_2O_4: even in the middle of (010) faces, only a few balls were observed, without any regular orientation (Fig. 5).

As such, AFM could not bring an undisputable proof of the assignment of the observed balls as coke. However, comparisons of the series of images with the speculated views elaborated on the basis of the literature strongly argue in that direction. First, the balls only appeared after the catalytic reaction. They were never detected on any fresh samples, showing that the balls are formed during the reaction. Second, the adherence of the balls with the surface of the MoO_3 was very weak. This undoubtedly discards the possibility that the features result from a surface reorganization of MoO_3 during the reaction. If this had been the case, reorganized microvolumes of MoO_3 would have grown in an intimate epitaxial interaction with the initial crystal, corresponding to a stronger adherence than observed. On the other hand, previous investigations on $MoO_3 + Sb_2O_4$ mixtures in the same reaction have undoubtedly discarded the occurrence of mixed Mo–Sb–O or Mo–C–O phases to which the balls could in principle also have been assigned (15). Another point is the big difference between the number of balls and their organization in parallel rows detected in the middle of the (010) faces and on the edges where they meet the (100) faces. Under the hypothesis that the balls are coke, this observation is completely consistent with the distribution of the coke as predicted from the "structural specificities" of MoO_3 (8–12): the closer the edges with the (100) faces, the lower the amount of coke expected and the more disturbed their organization in parallel rows. Our other observation was that the number of balls was systematically smaller on MoO_3 used in the presence of antimony oxide than on MoO_3 reacted alone. In turn, under the hypothesis that the balls are coke, the observation is in total agreement with the inhibiting effect of α-Sb_2O_4 on the formation of coke in selective oxidation reactions (13, 14).

It is striking that there is a good correlation between the predictions of the presence of coke or not on some samples and the detection or not by AFM of large organized amounts of balls. This strongly supports the identification of the balls as coke deposits.

Even as a nonanalytical technique, AFM allowed the identification of coke deposits on the surface of MoO_3 crystals used as partial oxidation catalysts. These are balls of 10 nm diameter, organized in rows parallel to the [101] direction of the crystals. The identification was ascertained by systematic comparisons with predictions, based on arguments from the literature, whether coke should be present on some samples, and the AFM images of these samples. A good correlation has been obtained. AFM also appeared as a new tool for gently cleaning the surface of oxides. Even if performed at relatively low resolution, this investigation opens the possibility of new applications, where other techniques have failed until now, for atomic force microscopy in the field of catalyst imaging.

ACKNOWLEDGMENTS

The Fonds National de la Recherche Scientifique of Belgium is gratefully acknowledged for the fellowship and the "Crédit pour bref séjour à l'étranger" awarded to Eric Gaigneaux.

REFERENCES

1. Borko L., Nagy I., Schay, Z., and Guczi, L., *Appl. Catal. A* **147**, 95 (1996).

2. Podrebarac, G. G., Ng, F. T. T., and Rempel, G. L., *Appl. Catal. A* **147**, 159 (1996).
3. Laurent, E., Centeno, A., and Delmon, B., *Stud. Surf. Sci. Catal.* **88**, 573 (1994).
4. Larsson, M., Hulten, M., Blekkan, E. A., and Andersson, B., *J. Catal.* **164**, 44 (1996).
5. Bauer, F., Ernst, H., Geidel, E., and Schödel, R., *J. Catal.* **164**, 146 (1996).
6. McIntyre, B. J., Salmeron, M., and Somorjai, G. A., *J. Catal.* **164**, 184 (1996).
7. Trimm, D. L., *in* "Progress in Catalyst Deactivation" (J. L. Figueiredo, Ed.), p. 65. Nijhoff, The Hague/Boston/London, 1982.
8. Tatibouet, J. M., and Germain, J. E., *J. Catal.* **72**, 375 (1981).
9. Hernandez, R. A., and Ozkan, U. S., *Ind. Eng. Chem. Res.* **29**, 1454 (1990).
10. Brückman, K., Grabowski, R., Haber, J., Mazurkiewicz, A., Sloczyniski, J., and Wiltowski, T., *J. Catal.* **104**, 71 (1987).
11. (a) Mingot, B., Floquet, N., Bertrand, O., Treilleux, M., Heizmann, J. J., Massardier, J., and Abon, M., *J. Catal.* **118**, 424 (1989) 424; (b) Abon, M., Massardier, J., Mingot, B., Volta, J. C., Floquet, N., and Bertrand, O., *J. Catal.* **134**, 542 (1992).
12. (a) Volta, J. C., and Moraweck, B., *J. Chem. Soc. Commun.*, 338 (1980); (b) Volta, J. C., Desquenes, W., Moraweck, B., and Coudurier, G., *Kinet. Catal. Lett.* **12**, 241 (1979).
13. Li, C., Xin, Q., Ruiz, P., Guo, X. X., and Delmon, B., *J. Mol. Catal.* **72**, 307 (1992).
14. Zhou, B., and Delmon, B., *in* "2nd Conference on Spillover, June 12–16, 1989, Leipzig, Germany" (K.-H. Steinberg, Ed.), p. 87. Karl-Marx-Universität, Leipzig, Germany, 1989.
15. Weng, L.-T., and Delmon, B., *Appl. Catal. A* **81**, 141 (1992).